



ELSEVIER

Available online at www.sciencedirect.com

SCIENCE @ DIRECT®

Journal of Contaminant Hydrology 79 (2005) 67–88

JOURNAL OF

Contaminant
Hydrology

www.elsevier.com/locate/jconhyd

Hydrochemical and isotopic effects associated with petroleum fuel biodegradation pathways in a chalk aquifer

Michael J. Spence^a, Simon H. Bottrell^{b,*}, Steven F. Thornton^a,
Hans H. Richnow^c, Keith H. Spence^b

^aGroundwater Protection and Restoration Group, Department of Civil and Structural Engineering,
University of Sheffield, Mappin Street, Sheffield S1 3JD, UK

^bSchool of Earth Sciences, University of Leeds, Leeds LS2 9JT, UK

^cUFZ-Leipzig Halle GmbH, Permoser Strasse 15, 04318 Leipzig, Germany

Received 2 July 2004; received in revised form 28 April 2005; accepted 5 June 2005

Abstract

Hydrochemical data, compound specific carbon isotope analysis and isotopic enrichment trends in dissolved hydrocarbons and residual electron acceptors have been used to deduce BTEX and MTBE degradation pathways in a fractured chalk aquifer. BTEX compounds are mineralised sequentially within specific redox environments, with changes in electron acceptor utilisation being defined by the exhaustion of specific BTEX components. A zone of oxygen and nitrate exhaustion extends approximately 100 m downstream from the plume source, with residual sulphate, toluene, ethylbenzene and xylene. Within this zone complete removal of the TEX components occurs by bacterial sulphate reduction, with sulphur and oxygen isotopic enrichment of residual sulphate ($\epsilon_s = -14.4\text{‰}$ to -16.0‰). Towards the plume margins and at greater distance along the plume flow path nitrate concentrations increase with $\delta^{15}\text{N}$ values of up to $+40\text{‰}$ indicating extensive denitrification. Benzene and MTBE persist into the denitrification zone, with carbon isotope enrichment of benzene indicating biodegradation along the flow path. A Rayleigh kinetic isotope enrichment model for ^{13}C -enrichment of residual benzene gives an apparent ϵ value of -0.66‰ . MTBE shows no significant isotopic enrichment ($\delta^{13}\text{C} = -29.3\text{‰}$ to -30.7‰) and is isotopically similar to a refinery sample ($\delta^{13}\text{C} = -30.1\text{‰}$). No significant isotopic variation in dissolved MTBE implies that either the magnitude of any biodegradation-induced isotopic fractionation is

* Corresponding author. Tel.: +44 113 3435228; fax: +44 113 3435259.

E-mail address: simon@earth.leeds.ac.uk (S.H. Bottrell).

small, or that relatively little degradation has taken place in the presence of BTEX hydrocarbons. It is possible, however, that MTBE degradation occurs under aerobic conditions in the absence of BTEX since no groundwater samples were taken with co-existing MTBE and oxygen. Low benzene $\delta^{13}\text{C}$ values are correlated with high sulphate $\delta^{34}\text{S}$, indicating that little benzene degradation has occurred in the sulphate reduction zone. Benzene degradation may be associated with denitrification since increased benzene $\delta^{13}\text{C}$ is associated with increased $\delta^{15}\text{N}$ in residual nitrate. Re-supply of electron acceptors by diffusion from the matrix into fractures and dispersive mixing is an important constraint on degradation rates and natural attenuation capacity in this dual-porosity aquifer.

© 2005 Published by Elsevier B.V.

Keywords: MTBE; BTEX; Chalk; Groundwater; Biodegradation; Natural attenuation; Isotopes

1. Introduction

Even small releases of petroleum hydrocarbons into aquifers can lead to concentrations of dissolved hydrocarbons far in excess of regulatory limits. Conventional approaches to groundwater remediation (e.g. pump and treat) can be disproportionately costly, particularly for small or diffuse groundwater contamination plumes, and there may be restrictions on their application, especially in urban areas. On this basis monitored natural attenuation (NA) is often proposed as an alternative means of managing the risk associated with sub-surface contamination. This approach does, however, require a good understanding of the processes that underpin the NA option. In the case of petroleum fuel contamination, it is particularly important to understand the behaviour of benzene (due to its toxicity and carcinogenic properties) and ether oxygenates (e.g. methyl-tert-butyl ether, MTBE, due to their low taste and odour threshold and low biodegradation potential). The behaviour of these components can be crucial to the effectiveness of NA as a remediation option for petroleum hydrocarbon contamination in groundwater.

To date, the majority of studies assessing the in-situ biodegradation of BTEX and ether oxygenates have been completed in shallow, unconfined aquifers in unconsolidated sediments. Conclusions from these studies are not directly applicable to biodegradation occurring in deeper fractured bedrock aquifers, such as the Chalk, which is a major groundwater resource in southern and eastern England and parts of north-west mainland Europe. This study provides an improved understanding of biodegradation processes for dissolved petroleum hydrocarbon compounds in the Chalk aquifer, particularly rates and limitations on degradation potential, which are fundamental to the evaluation of NA performance in this system. The study is based on an unleaded fuel spill and focuses on the fate of two key components, benzene and MTBE, as representative compounds with different properties in the hydrocarbon mixture.

Whereas sorption processes reduce dissolved contaminant concentrations and retard contaminant migration relative to groundwater, biodegradation reduces total contaminant mass in the groundwater system. When the rate of contaminant biodegradation in the

groundwater equals the rate of contaminant supply the contaminant plume is said to be in steady state. Rates of degradation in excess of contaminant supply will lead to a shrinking plume. Understanding biodegradation processes and controls on their rates for different contaminants in a plume is therefore central to assessing the aquifer capacity for NA. For petroleum fuel hydrocarbons, biodegradation proceeds via a series of microbially-mediated respiration reactions using different electron acceptors in the aquifer. These electron acceptors are often utilized in a sequence dictated by their relative energy yields per unit of organic carbon oxidized (e.g. Chapelle et al., 1995; Lyngkilde and Christensen, 1992; Postma and Jakobsen, 2000; Thornton et al., 2001), in the following order: O₂, NO₃⁻, Mn(IV), Fe(III), SO₄²⁻ (Table 1). The contribution of each electron acceptor in degradation depends on its availability in the aquifer and the ability of the indigenous microorganisms to utilize it. Under highly anaerobic conditions, fermentation of organic contaminants to methane can also occur (Chapelle et al., 1995; Thornton et al., 2001).

The Chalk aquifer is a dual porosity system with a highly porous (ca. 30–40%) rock matrix and a well-developed fracture network. Most (~99%) of the groundwater is present as interstitial water in the matrix pore-space, although the fracture network dominates groundwater flow and inputs to monitoring wells. Contaminants released into the saturated zone of the aquifer will initially enter the fracture system, where high flow velocities can increase contaminant migration rates. However, contaminant migration is influenced by diffusion between mobile groundwater in the fractures and immobile, uncontaminated groundwater in the matrix. Conversely, the uncontaminated matrix can provide a significant reservoir of dissolved electron acceptors for potential biodegradation reactions. The significance of these different (physical and biological) processes and their influence on NA in a dual-porosity aquifer are not well understood and form a key aspect of this study.

In this paper we examine the distribution and isotopic composition of petroleum fuel contaminants, electron acceptors (nitrate, sulphate) and dissolved inorganic carbon in groundwater of the Chalk aquifer beneath a petroleum hydrocarbon spill site in southern England. The contamination arose from an unleaded fuel spill that has reached the saturated zone of the aquifer. The spatial distribution of dissolved contaminants and other chemical indicators of degradation processes in the aquifer has been assessed

Table 1
Terminal electron accepting processes for toluene oxidation

Microbial process	Degradation reactions for toluene (C ₇ H ₈)*	Reaction no.
Aerobic degradation	C ₇ H ₈ + 9O ₂ ⇒ 7CO ₂ + 4H ₂ O	1
Denitrification	5C ₇ H ₈ + 36NO ₃ ⁻ + H ⁺ ⇒ 35HCO ₃ ⁻ + 3H ₂ O + 18N ₂	2
Manganese(IV) reduction	C ₇ H ₈ + 18MnO ₂ + 29H ⁺ ⇒ 7HCO ₃ ⁻ + 18Mn ²⁺ + 15H ₂ O	3
Fe(III) reduction	C ₇ H ₈ + 36FeOOH + 65H ⁺ ⇒ 7HCO ₃ ⁻ + 36Fe ₂ ⁺ + 51H ₂ O	4
Sulphate reduction	2C ₇ H ₈ + 9SO ₄ ²⁻ + 6H ₂ O ⇒ 14HCO ₃ ⁻ + 5H ₂ S + 4HS ⁻	5
Methanogenesis	2C ₇ H ₈ + 10H ₂ O ⇒ 5CO ₂ + 9CH ₄	6

*:Electron acceptors are shown in bold.

using both single screen monitoring wells and multilevel sampling wells. We use carbon isotopic compositions of benzene and MTBE to investigate the in situ degradation of these compounds and carbon isotopic composition of total dissolved inorganic carbon, TDIC, ($\text{TDIC} = \text{CO}_3^{2-} + \text{HCO}_3^- + \text{H}_2\text{CO}_3 + \text{CO}_2 \text{ (aq)}$) to assess the impacts of contaminant mineralization on the groundwater TDIC budget. In addition to chemical indicators of groundwater redox status, isotopic compositions of sulphate, sulphide and nitrate are used to investigate whether sulphate and nitrate reduction are significant pathways for degradation of hydrocarbons in this aquifer. Importantly, we focus on establishing the conditions and factors controlling NA of benzene and MTBE in the Chalk aquifer.

2. Site overview

The study site is a former retail filling station located on the Chalk aquifer in southern England. The Chalk aquifer is overlain by ca. 11 m of Quaternary sediments, comprising predominantly sands and gravels. The upper part of the drift thickness has been variably affected by urbanization and up to 4m of made ground may be present. The aquifer is unconfined with an unsaturated zone thickness of ca. 20 m, so the piezometric surface lies entirely within the Chalk (Wealthall et al., 2002). In February 1999 ~55,000L of unleaded fuel escaped from an underground storage tank, contaminating the aquifer with petroleum hydrocarbons, including benzene, toluene, ethylbenzene, xylenes (BTEX), and the ether oxygenate compounds methyl tert-butyl ether (MTBE) and tert-amyl methyl ether (TAME). Treatment of the LNAPL source was carried out from 1999 to 2002 using a soil vapour extraction (SVE) system. Low vapour yields eventually led to its use being discontinued, although locally high BTEX and oxygenate concentrations in the unsaturated zone constitute a residual source of contaminated infiltration water to the deeper aquifer. In June 2002 the site was closed and in September 2002 six underground storage tanks were removed from the plume source zone.

The network of monitoring wells installed at the site to sample groundwater chemistry, determine dissolved contaminant distribution and assess NA is shown in Fig. 1. This network includes monitoring wells fitted with single screens (MW7, 9 and 13), where the screened interval extends from the water table approximately 10m into the saturated aquifer, and multilevel sampling wells (MLS) equipped with seven sample ports containing 10cm screens (Einarson and Cherry, 2002). Adjacent sample ports on the MLS are isolated using bentonite seals, which allow level-discrete sampling from up to seven depth intervals in one well. Groundwater flow at the site is toward the SSE in response to a regional-scale hydraulic gradient (~0.002), with water table fluctuations of $\pm 1.5\text{m}$ over a 4-year period (Fig. 1). The monitoring wells are, therefore, aligned approximately parallel to the direction of groundwater flow (Fig. 1). Eight MLS have been installed: one upgradient (MLS14), one beneath the source (MLS23), and 6 in the downgradient plume (MLS15–20) to characterise contaminant transport and NA processes in the aquifer (Fig. 1). Groundwater quality sampling has identified dissolved phase contamination between 20–30 m depth in the saturated zone,

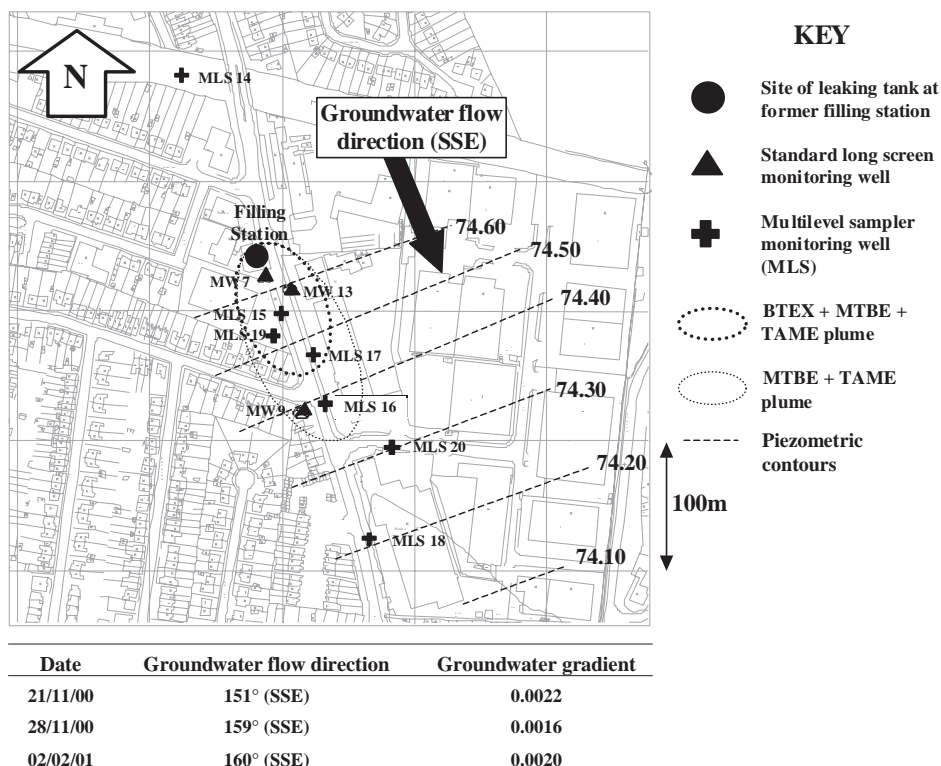


Fig. 1. Site map showing monitoring well locations, the former filling station, groundwater flow direction, piezometric contours (mAOD) and the approximate location of the mixed BTEX/oxygenate plume and the oxygenate plume.

with a mixed oxygenate/ BTEX plume close to the site and oxygenate-only plume further downgradient.

3. Materials and methods

3.1. Samples for chemical analysis

Groundwater was sampled in June/July 2002 using procedures that ensured the collection and preservation of anaerobic sample quality. These procedures included the use of a purpose built sample processing manifold equipped with a flowcell, which was connected directly to a dedicated inertial lift pump in each monitored level. Pressure filtration of samples was completed on-site with this apparatus, using N_2 . Each monitoring well was purged prior to sampling until wellhead parameters (electrical conductivity (E.C.), redox potential (Eh) and dissolved oxygen (D.O.)) stabilised. This purging protocol takes account of the volume of each chamber in the MLS. Time-series

Table 2
Procedures used for analysis of groundwater samples

Species	Analytical method	Method detection limit	Precision
Wellhead parameters: pH, Eh, D.O., E.C., temperature	Flowcell with dedicated probes	0.1 pH units, 1 mV, 0.1 mg/l, D.O., 1 μ S/cm, 0.1 $^{\circ}$ C	Recorded value represents stable reading on meter during sampling. Meters were calibrated prior to use using certified standards
Fuel hydrocarbons: BTEX, MTBE, TAME, TBA	EPA 624/8260 using mass-sensitive detection	1 ppb	5% RSD
Anions: F ⁻ , Cl ⁻ , Br ⁻ , NO ₃ ⁻ , NO ₂ ⁻ , SO ₄ ²⁻	Ion chromatography (Dionex DX 120 system)	0.05 mg/l	5% RSD
Dissolved gases: CO ₂ , CH ₄	Collected by equilibration with an N ₂ bubble in a gas flowcell (Thornton et al., 2001)	1 μ g/l	Recorded value is average of duplicate analyses
Sulphide: HS ⁻	Determined by nitrogen sparging of 20 l of acidified groundwater and quantitative recovery as Ag ₂ S	1 μ g/l	Not applicable
TDIC: Expressed as mg/l C	Determined quantitatively via CO ₂ yield from SrCO ₃ precipitate formed on addition of excess SrCl ₂	1 mg/l	Not applicable
Transition metals: Mn ²⁺ , Fe ²⁺	ICP-AES	0.01 mg/l	5% RSD

sampling of individual levels in the monitoring wells has confirmed that the sample chemistry rapidly stabilises within the purging time used and provides reproducible samples. Table 2 lists analytical methodologies used to determine the aqueous chemistry, together with the precision and detection limit for each analysis technique. All samples were transferred directly to appropriate sample bottles, which were filled completely to leave no headspace. This minimised contact with the atmosphere and stabilised the concentrations of reactive species. All groundwater samples were stored in an on-site chiller cabinet at 4 $^{\circ}$ C.

4. Isotopic analyses

4.1. Samples for isotopic analysis

Groundwater samples for the analysis of total dissolved inorganic carbon (TDIC) and $\delta^{13}\text{C}$ -TDIC were collected in airtight bottles and fixed as SrCO₃ by the addition of SrCl₂ ammonia (Bishop, 1990). Samples for isotopic analysis of SO₄-S ($\delta^{34}\text{S}$ -SO₄) and SO₄-O ($\delta^{18}\text{O}$ -SO₄) were collected in 0.5 litre dark glass bottles containing 1 g/l

sodium azide to limit microbial activity. The bottles were filled completely with groundwater, sealed with PTFE lined caps and stored in the dark at 4 °C prior to analysis. Samples for compound-specific carbon isotope analysis (CSIA) of benzene and MTBE were collected in 125 ml glass crimp vials containing 35 g of Analar sodium chloride, which were filled and sealed in the field, leaving a headspace of approximately 2 ml. PTFE faced butyl rubber septa were used to minimise analyte loss through sorption into the septum. Samples were stored inverted at 5 °C prior to analysis.

4.2. Recovery of pure barium sulphate and silver nitrate from groundwater samples for isotopic analysis

Samples were acidified to between pH 2.0 and 2.5 and heated to ~80 °C on a hot plate. A volume of 100 g/l BaCl₂ solution equal to 10% of the sample volume was then added and the BaSO₄ precipitate left to cool and coarsen overnight. Barium sulphate precipitates were recovered on 0.45µm cellulose nitrate membranes and washed with deionised water prior to drying at 50 °C. Nitrate was prepared as pure AgNO₃ following the method of Silva et al. (2000).

4.3. Nitrate, sulphate and sulphide stable isotope analysis

Nitrate and sulphur isotopic analyses were performed on a Micromass Isoprime continuous flow mass spectrometer coupled to a Eurovector Elemental Analyser. BaSO₄ and Ag₂S were weighed out in tin cups and converted to SO₂ by flash combustion at 1020 °C in the presence of oxygen. Quantitative conversion to SO₂ was achieved by passing the gases through tungstic oxide. Excess oxygen was removed by reaction with hot copper at about 650 °C. AgNO₃ for nitrogen isotope analysis was weighed out into silver cups and reduced to N₂ and CO by reaction with glassy carbon and a nickelised carbon catalyst at 1260 °C. The gas mixtures produced were separated on a GC column and the appropriate gas analysed for mass abundance. Method precision is better than 0.3‰ for δ³⁴S and better than 0.2‰ for δ¹⁵N.

The analysis of δ¹⁸O was achieved by converting SO₄ to CO₂ by reaction with graphite as described by McCarthy et al. (1998) with a precision of ± 0.4‰. δ¹⁸O determinations were carried out using a VG Sira-10 gas source mass spectrometer and the data corrected using standard procedures (Craig, 1957). Sulphur, carbon, nitrogen and oxygen isotope data are reported using the standard δ-notation (Eq. (1)), relative to the V-CDT, V-PDB, AIR and V-SMOW standards, respectively:

$$\delta^{13}\text{C} = \left[\frac{(^{13}\text{C}/^{12}\text{C})_{\text{sample}} - (^{13}\text{C}/^{12}\text{C})_{\text{standard}}}{(^{13}\text{C}/^{12}\text{C})_{\text{standard}}} \right] \times 1000 \quad (1)$$

where $(^{13}\text{C}/^{12}\text{C})_{\text{sample}}$ and $(^{13}\text{C}/^{12}\text{C})_{\text{standard}}$ are the isotopic ratio in sample and standard, respectively.

4.4. TDIC quantification and carbon isotopic analysis of TDIC and bulk organic carbon samples

Total dissolved inorganic carbon ($\text{CO}_3^{2-} + \text{HCO}_3^- + \text{H}_2\text{CO}_3 + \text{CO}_{2(\text{aq})}$) was recovered from a known mass of groundwater by precipitation with alkaline SrCl_2 solution (Bishop, 1990). The precipitate of impure strontium carbonate was then recovered on a $0.45\text{-}\mu\text{m}$ cellulose nitrate membrane and dried at $50\text{ }^\circ\text{C}$. The total precipitate mass was noted and a sub-sample taken for conversion to CO_2 in a high vacuum line. The CO_2 yield from this process was then used to calculate the groundwater TDIC from the precipitate mass. CO_2 gas for isotopic analysis was produced from organic compounds by combustion in sealed quartz tubes as described by Louie et al. (1993). $\delta^{13}\text{C}$ determinations on samples of CO_2 gas were carried out using a VG Sira-10 gas source mass spectrometer and the data corrected using standard procedures and are reported relative to the V-PDB standard. Precision is better than 0.05‰ .

4.5. Compound specific carbon isotope analysis of oxygenate/BTEX components

Carbon isotope ratios were determined using an Agilent 6890A gas chromatograph coupled through a combustion interface and water trap to a Finnigan MAT 252 continuous flow irMS. A 60m RTX-5 (integrated guard) column was used with an internal diameter of 0.32 mm and a film thickness of $0.5\text{ }\mu\text{m}$. Repeat analyses of headspace gas were found to yield an analytical precision (95% confidence interval) of $\pm 0.6\text{‰}$ for benzene and $\pm 0.3\text{‰}$ for MTBE. The detection limit of the technique was $\sim 1\text{ }\mu\text{g/l}$ for benzene and $\sim 10\text{ }\mu\text{g/l}$ for MTBE. Peak separation in the GC was optimal for groundwater samples bearing relatively few analytes, and hence the technique was particularly appropriate for samples containing

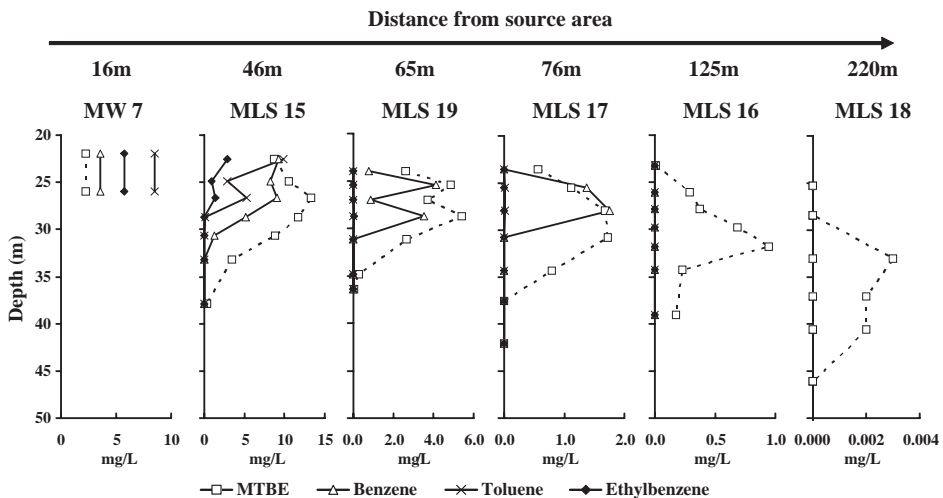


Fig. 2. Distribution of selected contaminant species in groundwater at multilevel sampling wells.

only residual benzene and oxygenates. Samples from close to the plume source generated a high background signal in the irMS, yielded less reliable analyses, and are not reported.

5. Results and discussion

5.1. Distribution of contaminants within the plume

Fig. 2 shows the distribution of selected dissolved hydrocarbons in groundwater along the plume flow path, to illustrate the general behaviour of different contaminant groups.

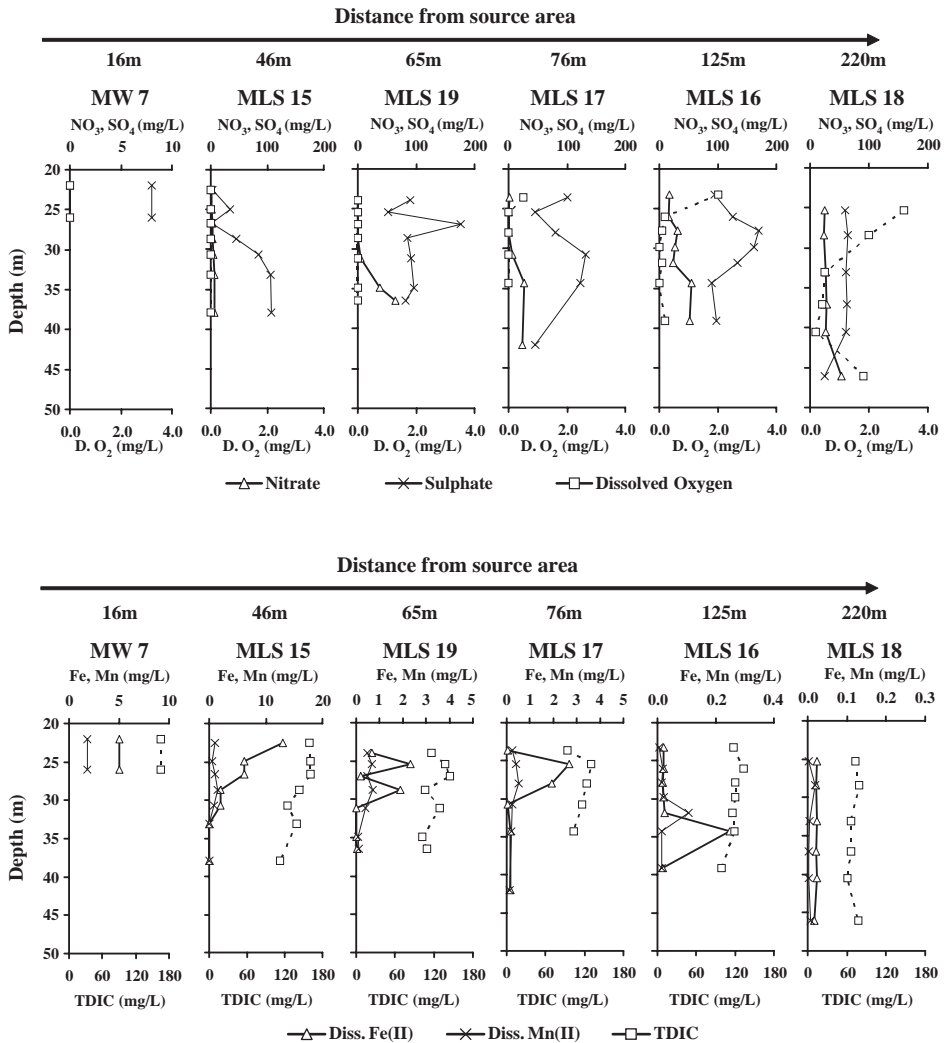


Fig. 3. Distribution of electron acceptors and other species in groundwater at multilevel sampling wells.

Table 3
Concentration and isotopic data for samples collected in June/July 2002

Sample ID	Nitrate		Sulphate			TDIC		Sulphide		Methane
	mg/l	$\delta^{15}\text{N}$	mg/l	$\delta^{34}\text{S}$	$\delta^{18}\text{O}$	mg/l	$\delta^{13}\text{C}$	mg/l	$\delta^{34}\text{S}$	mg/l
MW7	na	na	60.7	22.2	12	112.9	21.6	0.525	-5.7	<0.001
MW9	51.1	11.7	109.8	4.6	3.8	128.4	-15.7	0.000	na	0.041
MW13	na	na	7.9	23.3	11.6	161.5	-20.2	1.540	-3.2	<0.001
MLS 14/2	54.5	9.2	133.3	1.9	8.8	69.0	-14.7	<0.001	na	<0.001
MLS 14/3	75.6	10.1	145.9	1.6	7.6	74.0	-14.7	<0.001	na	<0.001
MLS 14/4	104.5	12.8	109.5	2.3	na	102.5	-14.9	<0.001	na	<0.001
MLS 14/5	72.7	na	41.8	1.9	4.8	97.9	-13.5	<0.001	na	<0.001
MLS 14/6	28.8	10.0	9.2	2.0	4.8	73.5	-14.7	<0.001	na	<0.001
MLS 14/7	40.7	9.1	11.2	5.4	4.5	75.2	-14.4	<0.001	na	0.114
MLS 15/1	<0.5	na	3.3	15.7	na	156.3	-20.9	0.282	12.9	0.161
MLS 15/2	<0.5	na	34.0	22.6	11.1	158.4	-20.3	0.105	7.3	0.291
MLS 15/3	<0.5	na	0.9	na	na	158.8	-20.4	0.508	12.1	0.050
MLS 15/4	<0.5	na	45.3	14.4	9.9	139.6	-20.6	0.117	-6.2	0.028
MLS 15/5	<0.5	na	84.4	6.5	8.9	121.7	-18.5	0.023	-29.1	0.005
MLS 15/6	6.1	40.1	105.3	3.6	8.1	137.1	-17.2	0.001	na	0.001
MLS 15/7	45.6	15.5	107.8	2.5	3.4	110.6	-16.1	0.008	na	<0.001
MLS 16/1	17.3	9.9	94.5	4.7	7.8	116.6	-17.7	<0.001	na	<0.001
MLS 16/2	16.3	15.5	125.4	4.0	6.5	135.2	-18.2	<0.001	na	<0.001
MLS 16/3	30.8	13.6	170.5	3.9	5.0	123.6	-16.2	<0.001	na	<0.001
MLS 16/4	26.7	17.6	162.8	4.4	6.7	121.5	-18.2	<0.001	na	<0.001
MLS 16/5	24.4	16.8	133.8	4.1	6.8	118.0	-13.9	<0.001	na	<0.001
MLS 16/6	55.5	na	89.7	3.4	5.9	122.1	-17.9	<0.001	na	<0.001
MLS 16/7	52.3	12.1	97.1	3.1	4.4	100.6	-15.6	<0.001	na	<0.001
MLS 17/1	0.9	na	100.6	6.1	na	93.5	-18.6	<0.001	na	<0.001
MLS 17/2	0.0	na	46.4	18.5	11.7	127.7	-19.2	0.225	-21.3	<0.001
MLS 17/3	0.0	na	80.9	12.0	8.4	122.5	-19.7	0.051	-14.2	<0.001
MLS 17/4	5.5	na	132.4	4.7	7.9	114.4	-17.3	<0.001	na	<0.001
MLS 17/5	26.1	na	123.0	3.8	7.0	102.3	-16.1	<0.001	na	<0.001
MLS 17/7	23.8	na	45.8	na	na	na	na	na	na	<0.001
MLS 18/1	24.5	10.9	59.2	4.1	5.7	72.0	-14.3	<0.001	na	<0.001
MLS 18/2	22.8	na	63.8	4.3	na	77.5	-14.2	<0.001	na	<0.001
MLS 18/3	26.9	10.1	61.0	3.8	5.0	65.7	-16.2	<0.001	na	<0.001
MLS 18/4	27.7	9.9	62.9	3.8	na	65.2	-15.8	<0.001	na	<0.001
MLS 18/5	26.8	11.5	60.9	3.8	5.5	60.5	-16.1	<0.001	na	<0.001
MLS 18/6	53.2	9.8	25.1	2.2	3.1	78.5	-13.0	<0.001	na	<0.001
MLS 18/7	51.8	na	27.9	1.7	na	85.7	-13.3	<0.001	na	<0.001
MLS 19/1	0.0	na	89.1	11.4	10.9	114.4	-19.7	<0.001	na	<0.001
MLS 19/2	0.0	na	52.6	20.8	10.6	136.7	-20.7	0.075	na	0.205
MLS 19/3	0.0	na	176.2	8.2	9.2	141.2	-19.3	<0.001	na	0.221
MLS 19/4	0.0	na	84.4	8.5	12.4	104.3	-18.9	<0.001	na	0.234
MLS 19/5	4.3	20.1	92.0	4.7	7.6	128.2	-16.4	<0.001	na	0.009
MLS 19/6	38.5	16.6	96.8	3.5	5.6	100.2	-15.5	<0.001	na	0.004
MLS 19/7	63.9	12.2	82.5	3.0	3.6	107.0	-15.1	<0.001	na	0.002
MLS 20/1	11.1	na	76.5	2.1	4.6	81.9	-14.9	<0.001	na	<0.001
MLS 20/2	34.9	na	74.8	0.5	7.2	87.3	-13.7	<0.001	na	<0.001
MLS 20/4	37.5	na	17.2	3.4	3.5	63.4	-12.1	<0.001	na	<0.001
MLS 20/7	26.1	na	10.9	5.1	6.6	50.9	na	<0.001	na	<0.001

$\delta^{13}\text{C}$ data for MLS 14/2 is from the June 2003 dataset (this level was inadequately purged in 2002).

$\delta^{15}\text{N}$ data for MLS 15/6 and 15/7 taken from June 2001 dataset (no sample was taken in 2002).

The highest concentrations of dissolved hydrocarbons occur at MW7 and MLS15, close to the former filling station (Fig. 1). Comparison of data from monitoring wells located progressively downgradient shows that most hydrocarbons (e.g. toluene and ethylbenzene, Fig. 2) have a relatively restricted distribution. MLS19 has significantly lower concentrations of hydrocarbons, except benzene and MTBE, which are still present at relatively high concentration (max. 6 mg/l, Fig. 2). At MLS16 the dominant contaminant is MTBE (max. 1 mg/l) with only trace amounts of BTEX present (Fig. 2). At MLS18, which is the most downstream monitoring well, concentrations of MTBE are <10 ug/l. This distribution of contaminant concentration suggests that most hydrocarbons are attenuated in the “core” of the plume, within 50 m of the contaminant source, while benzene and the fuel oxygenates (MTBE, illustrated here, and also TAME) migrate further down the flow path.

5.2. Distribution of redox-sensitive species and redox zonation in groundwater

The plume exhibits a clear zonation in the concentrations of dissolved electron acceptors (O_2 , NO_3^- , SO_4^{2-}) and the products of contaminant biodegradation (TDIC, HS^- , Mn^{2+} , Fe^{2+}). Fig. 3 shows the distribution of these species in groundwater at the site. Methane is either below detection or present at low concentration (<0.3 mg L⁻¹; Table 3), indicating low levels of methanogenic activity within the plume. Up gradient of the site at MLS14 dissolved oxygen (D.O.) is present at concentrations up to 8 mg/l, with nitrate and sulphate concentrations ranging from 29–105 mg/l and 9–146 mg/l, respectively (Table 3). Close to the contaminant source, conditions in the plume are highly reducing; D.O., nitrate and sulphate have been removed and Fe(II) and Mn(II) are present in solution (Fig. 3, MW7, MLS15), as is HS^- (Table 3). Further downstream, at MLS16 and MW9, concentrations of dissolved electron acceptors increase and dissolved Fe, Mn and HS^- are no longer present. Concentrations of dissolved electron acceptors are close to background values at MLS18, the most downgradient monitoring well. TDIC concentrations in the downstream plume are elevated above those in the background aquifer, consistent with inputs of mineralised organic carbon from hydrocarbon biodegradation reactions.

6. Stable isotopes

6.1. Carbon isotopes in residual benzene and MTBE

Most components of the petroleum fuel spill are attenuated within 50 m of the source area, with the notable exception of the ether oxygenates and benzene, which have migrated ~115m down the flow path to MLS16 (Figs. 1 and 2). These compounds may degrade given sufficient time, so it is important to determine whether degradation is occurring and to estimate rates in order to predict the longevity of the plume.

During degradation, both benzene and MTBE may become enriched in ¹³C as bacteria selectively degrade molecules containing the lighter isotope of carbon (¹²C). Reported carbon isotopic enrichment factors for the biodegradation of benzene typically range from -1.5 ‰ to -3.6 ‰ under both aerobic and anaerobic conditions (Hunkeler et al., 2001a;

Mancini et al., 2003; Bottrell and Spence, 2003). For MTBE the aerobic isotopic enrichment factor is typically around -2‰ for aerobic degradation and -13‰ for anaerobic degradation (Hunkeler et al., 2001b; Kuder et al., 2005). Enrichment in ^{13}C could in principle, therefore, provide positive evidence for in-situ biodegradation of these hydrocarbons. Groundwater samples from the plume were analysed by GC-irMS to determine the carbon isotope ratios of residual benzene and MTBE. Fig. 4 shows the variation in the carbon isotope ratios of benzene and MTBE with depth at MLS15 and 16. The error bars represent 95% confidence intervals, calculated from replicate analyses of each sample. At both MLS15 and 16 the carbon isotope ratio of residual MTBE is approximately constant (-30.7‰ to -29.3‰) and shows no significant variation with depth. Isotopic analysis of pure MTBE from a refinery supplying unleaded fuel to the filling station yielded a $\delta^{13}\text{C}$ of -30.1‰ , which falls within this measured range. No significant isotopic variation in the MTBE implies that either the magnitude of any biodegradation-induced isotopic fractionation is small, or that relatively little degradation has occurred in the plume.

Data for benzene (Fig. 4) show a much greater range in $\delta^{13}\text{C}$ (-30.17‰ to -23.75‰). The lightest (i.e. undegraded) isotopic compositions occur within 5 m of the water table at

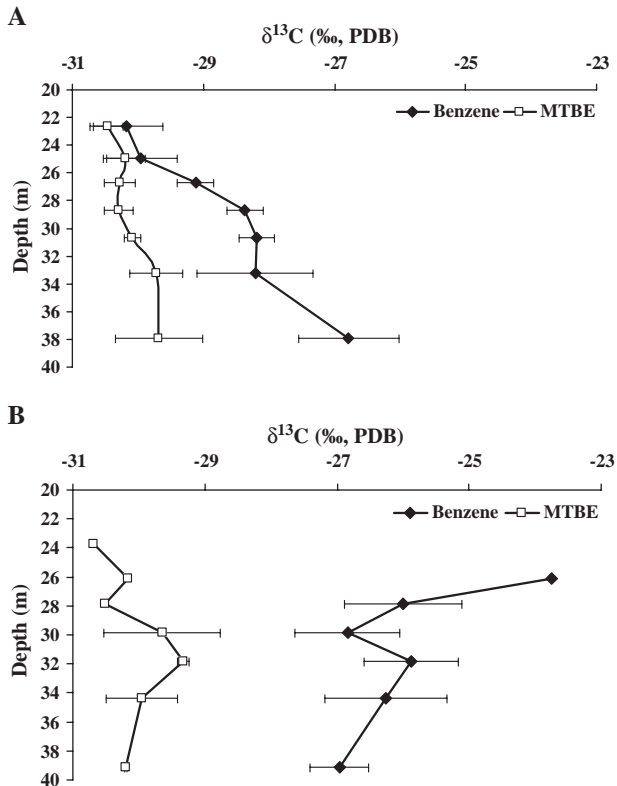


Fig. 4. Carbon isotopic composition versus depth for benzene and MTBE in groundwater samples from (A) MLS15 (30 m from source); and (B) MLS16 (115 m from source).

MLS15 (-30.17‰ , -29.96‰), coincident with the highest measured benzene concentrations (8–9 mg/l). With increasing depth at MLS15 (Fig. 4), and distance down the flow path (cf. MLS15 vs. MLS16, Fig. 4) $\delta^{13}\text{C}_{(\text{benzene})}$ increases while benzene concentrations decrease. Enrichment of residual benzene in ^{13}C is greatest where concentrations of other BTEX components are close to zero. This can be seen by reference to Figs. 2 and 4: where toluene and ethylbenzene are present at >0.1 mg/l (MLS15/1, 15/2 and 15/3) $\delta^{13}\text{C}_{(\text{benzene})}$ is within 1‰ of its lightest measured value (-29.1‰ to -30.1‰). The observations outlined above are consistent with benzene biodegradation in the outer margin of the downstream plume. The primary control on degradation appears to be the exhaustion of other, more favourable substrates including toluene and ethylbenzene, which is related to electron acceptor availability.

At MLS16 similar conditions prevail to those found in the deeper part of the aquifer ($>34\text{m}$) at MLS15; i.e. only oxygenates and benzene remain, and electron acceptors are abundant. Trace benzene (~ 1 ppb) was found to be isotopically heavy ($>-26\text{‰}$), consistent with the results from MLS15, and indicative of continued degradation of benzene down the flow path. A plot of $\delta^{13}\text{C}$ vs. natural logarithm of benzene concentration for MLS15 and 16 shows a trend of increasing $\delta^{13}\text{C}$ with decreasing

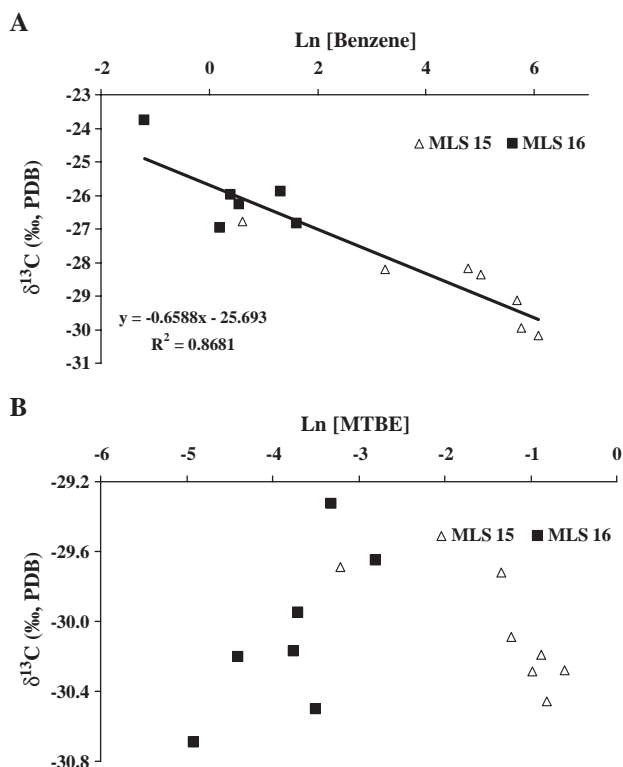


Fig. 5. Carbon isotopic composition versus natural logarithm of analyte concentration for (A) benzene and (B) MTBE in groundwater samples from MLS15 and MLS16.

concentration, this being due to a combination of degradation and dilution (Fig. 5). Assuming no dilution, and the same initial benzene concentration and carbon isotope ratio in all samples, Eq. (2) may be used to obtain a pseudo-Rayleigh isotopic enrichment factor (ϵ) for benzene degradation:

$$\delta^{13}\text{C}_{\text{residue}} = \delta^{13}\text{C}_{\text{initial}} + \epsilon \ln(C/C_0) \quad (2)$$

where $\delta^{13}\text{C}_{\text{residue}}$ is the carbon isotope ratio in residual benzene (‰), $\delta^{13}\text{C}_{\text{initial}}$ is the initial carbon isotope ratio of benzene prior to degradation (‰), ϵ is the isotopic enrichment factor (‰), C_0 is the initial benzene concentration and C is the residual benzene concentration.

From the parameters of the regression line shown on Fig. 5, $\epsilon = -0.66\text{‰}$. This is significantly lower than values obtained in microcosm studies (-1.5‰ to -3.6‰ ; Hunkeler et al., 2001a, Mancini et al., 2003) and implies that large changes in concentration produce relatively little isotopic effect. Assuming that the true value of ϵ is closer to that measured in microcosm studies (e.g. -2‰), it follows that 80% of the concentration reduction is due to processes other than degradation (e.g. dilution, adsorption).

A similar Rayleigh plot for MTBE shows only scatter (Fig. 5) and all the MTBE isotopic compositions fall around the value analysed in the source MTBE (-30.1‰). Hence, changes in the $\delta^{13}\text{C}$ of benzene give a good indication that active biodegradation of benzene is occurring, but there is no evidence to support MTBE degradation *within* the BTEX plume.

6.2. Nitrogen isotope data

Low or zero nitrate concentrations in the plume source compared to 29–105 mg/l in the upstream borehole MLS14 (Table 3; Fig. 3) indicate that denitrification is taking place in the contaminant plume. Levels 1–5 at MLS15 contain too little nitrate to permit isotopic analysis. MLS15/6 has 6.1 mg/l NO_3^- with a $\delta^{15}\text{N}$ of $+40.1\text{‰}$ (2001 data, cf. Table 3), compared with 9–12‰ at the upstream borehole MLS14 (Fig. 6). The ^{15}N enrichment is characteristic of microbial utilization of NO_3^- as an electron acceptor, since denitrifying bacteria preferentially utilize $^{14}\text{NO}_3^-$ (Bottcher et al., 1990; Hubner, 1986; Mariotti et al., 1981). Nitrate at MLS15/7 is present at concentrations close to background (45.6 mg/l) and is less ^{15}N enriched ($+15.5\text{‰}$), indicating less denitrification. Above 35 mbgl at MLS16, where nitrate concentrations are depleted to ~50% of background values there is ^{15}N enrichment associated with the residual contaminant plume ($\delta^{15}\text{N}$ in the range 15–18‰, Fig. 6). At the furthest downstream well, MLS18, the $\delta^{15}\text{N}$ of nitrate is $<12\text{‰}$, reflecting lighter background values in the aquifer.

6.3. Sulphur and oxygen isotope data

Low sulphate concentration and the presence of dissolved sulphide close to the plume source (Fig. 3, Table 3) are indicative of bacterial sulphate reduction, driven by the oxidation of BTEX and other biodegradable components within the plume. This process results in preferential consumption of sulphate molecules containing the lighter (^{32}S)

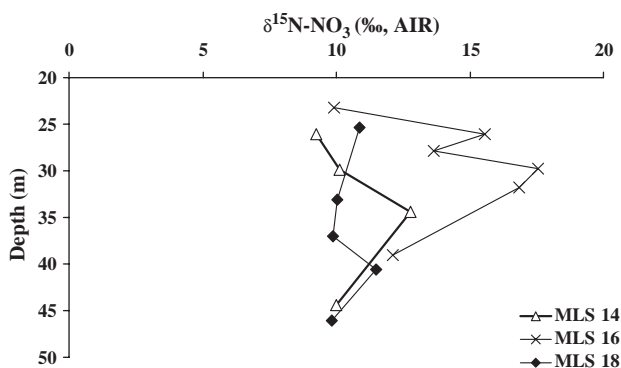


Fig. 6. Profiles of variation in $\delta^{15}\text{N-NO}_3$ for upstream (MLS14), plume (MLS16) and far downstream (MLS18) boreholes.

isotope of sulphur, partitioning ^{34}S into residual sulphate (Chambers and Trudinger, 1979; Strebel et al., 1990). The effects of this process are clearly apparent close to the plume source (boreholes MW7, MW13 and parts of MLS15, 17 and 19). Here the maximum $\delta^{34}\text{S}$ of residual sulphate is in the range of 18–22‰, whereas the $\delta^{34}\text{S}$ of sulphate in uncontaminated groundwater is less than 5‰ (Table 3, Fig. 7). Further downstream, at MLS16, sulphate $\delta^{34}\text{S}$ is similar to background values (Fig. 7). Dissolved sulphide is always isotopically light relative to co-existing sulphate, with $\delta^{34}\text{S}$ ranging from 12.9‰ to -29.1 ‰ (Table 3), again consistent with bacterial sulphate reduction. Sulphate reduction also enriches residual sulphate in ^{18}O (Fritz et al., 1989; Mizutani and Rafter, 1969) and a positive correlation exists between $\delta^{18}\text{O}$ and $\delta^{34}\text{S}$ in the sulphate (population correlation coefficient=0.73, Fig. 8). The isotopic evidence therefore clearly indicates that sulphate reduction is actively occurring in the contaminant plume, primarily within the zone of BTEX contamination.

Depth profiles of sulphate isotopic composition at MLS15, 17 and 19 (Fig. 7) show strong enrichment in ^{34}S , and hence extensive sulphate reduction, in the upper parts of the

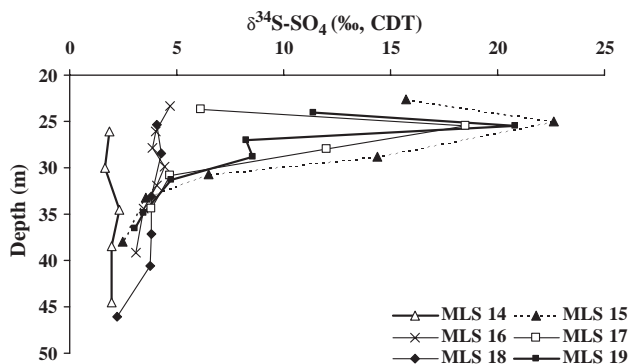


Fig. 7. Profiles of variation in $\delta^{34}\text{S-SO}_4$ at MLS boreholes along the plume flow path.

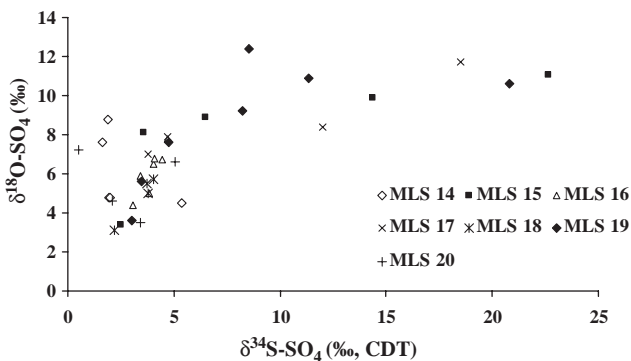


Fig. 8. Trends in sulphur and oxygen isotopic enrichment of dissolved sulphate at MLS boreholes along the plume flow path (population correlation coefficient=0.73).

monitored profile where contaminant (BTEX) concentrations are high. Assuming a closed system, and uniform initial sulphate concentration and isotopic composition, a plot of $\delta^{34}\text{S}$ vs. $\text{Ln}[\text{SO}_4]$ yields the isotopic enrichment factor, ϵ (Fig. 9 and Eq. (3)).

$$\delta^{34}\text{S}_{\text{residual sulphate}} = \delta^{34}\text{S}_{\text{initial sulphate}} + \epsilon \ln(C/C_0) \tag{3}$$

where $\delta^{34}\text{S}_{\text{residual sulphate}}$ is the sulphur isotope ratio in residual sulphate (‰), $\delta^{34}\text{S}_{\text{initial sulphate}}$ is the initial sulphur isotope ratio of sulphate prior to degradation (‰), ϵ is the isotopic enrichment factor (‰), C_0 is the initial sulphate concentration and C is the residual sulphate concentration.

From the gradient of the regression lines ϵ values of -14.4 , -16.0 ‰ are obtained for MLS 15 and 17, respectively. These are consistent with other estimates for sulphate reduction in fresh organic-rich groundwaters (-9.7 ‰, (Strebel et al., 1990); -9.8 ‰ (Bottrell et al., 1995); -9.9 ‰ (Spence et al., 2001)). Further downgradient at MLS19 sulphate concentrations are not depleted below background values and sulphide concentrations are extremely low (Table 3). Data from this monitoring well show no

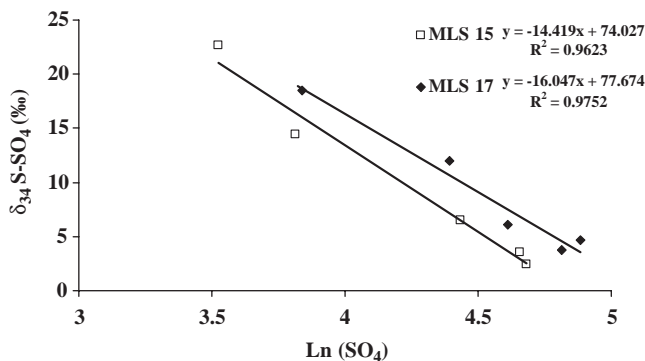
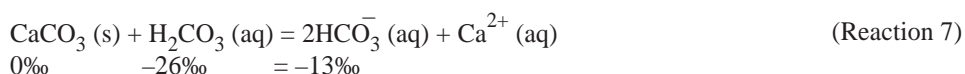


Fig. 9. Sulphate $\delta^{34}\text{S}$ versus natural logarithm of sulphate concentration at MLS15 and 17. The gradient of the regression lines gives an approximate value for the isotopic enrichment factor ϵ .

obvious correlation ($R^2=0.27$) between $\delta^{34}\text{S}$ and $\ln(\text{SO}_4)$ because here the fraction of sulphate reduced is insignificant.

6.4. Carbon isotopes in TDIC

The background concentration and isotopic composition of TDIC upstream of the plume range from 85 to 125 mg/l (MLS14, Table 3) and -13‰ to -16‰ (Fig. 10), respectively. These values result from reactions between carbonic acid produced by bacterial and plant respiration in the soil (isotopically light at $\sim -26\text{‰}$) and calcium carbonate in the Chalk matrix (at 0‰). In a calcareous aquifer, the production of carbonic acid by degradation reactions leads to rapid dissolution of calcium carbonate according to the following stoichiometry:



Chalk soil organic carbon

Thus the product bicarbonate is a 50:50 mix of carbon from the oxidised organic matter, and inorganic carbon derived from the Chalk. The numbers below the equation show the isotopic effect of the dissolution reaction since fractionation on dissolution of solid carbonate is insignificant. Lighter values, down to $\sim -16\text{‰}$, can be produced by partial equilibration with atmospheric CO_2 during this process (e.g. Boutton, 1991). These natural processes can thus explain the range of TDIC- $\delta^{13}\text{C}$ observed in the “background” groundwater at MLS14.

At MLS15, close to the plume source, TDIC increases to 163 mg/l and at MLS16, further downstream, it is still elevated at 146 mg/l (Fig. 3). This elevation is consistent with TDIC production through organic carbon oxidation. At both MLS15 and 16 TDIC concentrations are greater within the zone of contamination (22–30m), falling to background values at depth (Fig. 3).

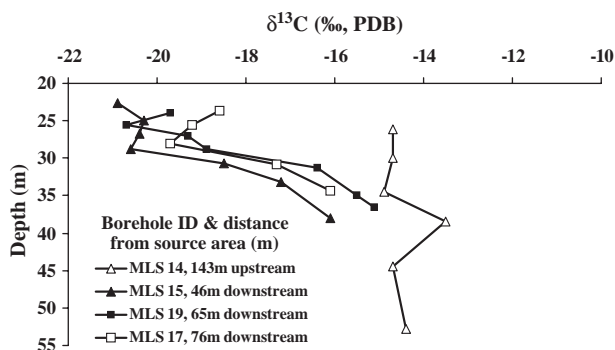


Fig. 10. Profiles of variation in $\delta^{13}\text{C}$ -TDIC showing progressive enrichment in ^{13}C , derived from hydrocarbon oxidation, closer to the plume source.

The carbon isotope ratio of the TDIC is significantly different downstream of the plume source (Fig. 10). At MLS15 the $\delta^{13}\text{C}$ of TDIC falls to around -21‰ within the plume, compared to a background value of -13‰ to -16‰ at MLS14. Further downstream at MLS16 the effect is less pronounced, with $\delta^{13}\text{C}$ values around -19‰ . The negative shift in $\delta^{13}\text{C}$ within the plume is consistent with the addition of isotopically light inorganic carbon to the groundwater, via oxidation of contaminant hydrocarbons ($\delta^{13}\text{C}_{(\text{unleaded fuel})} = -29.7\text{‰}$ to -29.9‰).

The products of organic carbon oxidation vary according to the process involved. Aerobic oxidation leads solely to the production of CO_2 (Reaction 1, Table 1) and thus carbonic acid. This reaction will produce dissolution of the Chalk matrix (Reaction 7) and yield bicarbonate with an overall isotopic composition of $\sim -13\text{‰}$. This is indistinguishable from the background (MLS14) and so would not produce the negative shifts in $\delta^{13}\text{C}$ observed at MLS15 and 16. However, most anaerobic processes, e.g. bacterial sulphate reduction, iron reduction, denitrification produce dominantly or solely alkaline bicarbonate (see Reactions 2, 3, 4 and 5; Table 1) and, e.g. for ethylbenzene:



Thus sulphate reduction and denitrification would add isotopically light carbon to the TDIC pool as bicarbonate, without lowering pH and inducing carbonate dissolution.

7. Synthesis

Sulphate $\delta^{34}\text{S}$ is a sensitive indicator of the extent of sulphate reduction in the plume (with increased $\delta^{34}\text{S}$ indicating a larger degree of sulphate reduction). Fig. 11 shows a plot of $\delta^{13}\text{C}$ of TDIC vs. $\delta^{34}\text{S}$ of sulphate for all samples. The data show a cluster (A on Fig. 11) with low $\delta^{34}\text{S}$ ($<5\text{‰}$) and $\delta^{13}\text{C}_{\text{TDIC}}$ between around -12‰ and -16‰ ; these are all

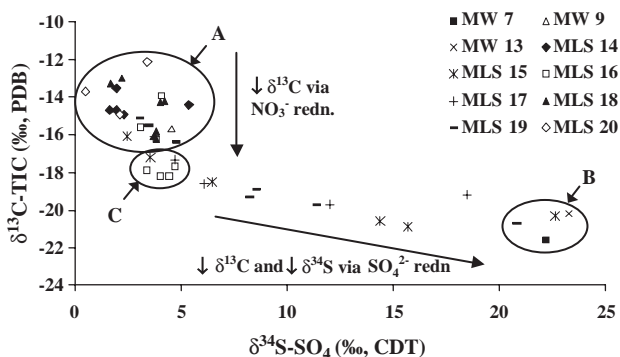


Fig. 11. Plot of $\delta^{13}\text{C}$ -TDIC versus $\delta^{34}\text{S}$ -sulphate for groundwater samples. Group A is uncontaminated and Group B is proximal to the contaminant spill. Elevated $\delta^{34}\text{S}$ indicates sulphate reduction, while depletion in $\delta^{13}\text{C}$ indicates addition of inorganic carbon via contaminant mineralization reactions. The figure delineates zones where sulphate reduction is dominant and zones where other biodegradation processes (principally denitrification) are the major contributors to TDIC (e.g. Group C)—see text.

locations that are remote from the core of the plume. Samples with high BTEX concentrations from close to the plume source have elevated $\delta^{34}\text{S}$ ($>20\text{‰}$) and $\delta^{13}\text{C}_{\text{TDIC}}$ of -20‰ to -25‰ (B on Fig. 11). There is also an array of data between group B and a grouping of data from MLS 16, labelled C on Fig. 11. The samples in this array are from monitoring points downgradient of, or vertically removed from, the plume core and are consistent with a mixing relationship between ^{34}S -enriched plume sulphate and background sulphate from outside the plume. Interestingly, although the group C data have almost no remaining shift in $\delta^{34}\text{S}$, they are still shifted to significantly lower $\delta^{13}\text{C}$ than the more remote “aquifer background” samples in group A. We attribute this apparently smaller degree of mixing with background TDIC (compared to sulphate) to the continued production of isotopically light TDIC by denitrification in the less-reducing outer part (fringe zone) of the plume. In this zone, concentrations of both nitrate and sulphate increase, and there is evidence for active denitrification (from the nitrate $\delta^{15}\text{N}$ profile) at MLS16 (Fig. 6). The rapid return of sulphate isotopic compositions to aquifer background values in the downstream part of the plume indicates that there must be either:

- (i) significant and rapid interaction between fracture waters and the dissolved electron acceptors present in the aquifer matrix; or
- (ii) dispersive mixing of contaminated fracture waters with groundwater from outside of the contaminant plume.

A plot of $\delta^{13}\text{C}$ of benzene against $\delta^{34}\text{S}$ of sulphate is presented in Fig. 12 for data from MLS15 and 16. Increasing $\delta^{13}\text{C}$ indicates progressive degradation of benzene, whereas high $\delta^{34}\text{S}$ indicates extensive sulphate reduction in the anaerobic core of the plume. Lower $\delta^{34}\text{S}$ indicates admixture with background groundwater sulphate. Low benzene $\delta^{13}\text{C}$ values correlate with high sulphate $\delta^{34}\text{S}$, showing that there is little benzene degradation in the sulphate reduction zone. Benzene $\delta^{13}\text{C}$ only increases to heavier compositions at lower values of sulphate $\delta^{34}\text{S}$, indicating that benzene degradation only occurs where other electron acceptors are mixed into the outer parts

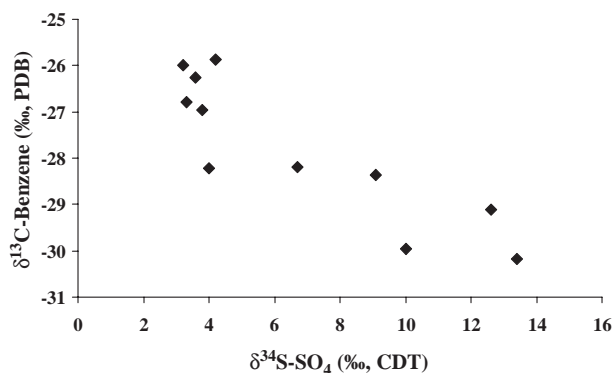


Fig. 12. Plot of $\delta^{13}\text{C}$ -benzene versus $\delta^{34}\text{S}$ -sulphate. Elevated $\delta^{34}\text{S}$ indicates sulphate reduction, while enrichment in $\delta^{13}\text{C}$ in residual benzene (i.e. less negative values of $\delta^{13}\text{C}$) indicates its biodegradation. Significant benzene degradation only occurs in samples from outside the sulphate reduction zone.

(fringe zone) of the plume, where nitrate reduction has been identified. Hence, while sulphate reduction is an important process overall for mineralization of hydrocarbon contaminants, it apparently plays little or no role in benzene degradation. Benzene degradation may be associated with nitrate reduction at the margins of the plume in the absence of other, more biodegradable, hydrocarbons (e.g. toluene, ethylbenzene) since increased benzene $\delta^{13}\text{C}$ is associated with increased $\delta^{15}\text{N}$.

Note that none of the monitoring wells allow us to investigate the outermost “halo” of the plume fringe where MTBE and O_2 will be present. Aerobic MTBE degradation may take place where mixing with uncontaminated groundwater re-establishes a sufficiently high dissolved oxygen concentration and other more biodegradable hydrocarbon compounds are absent.

8. Conclusions

This study has demonstrated a strong zonation in the contaminant plume with respect to both redox conditions and active biodegradation pathways. In an inner anaerobic zone, up to 50 m downgradient of the source area, biodegradation is dominated by bacterial sulphate reduction and nitrate is completely removed. In this zone many petroleum hydrocarbon compounds are mineralized, but benzene and MTBE are not significantly degraded (Fig. 13). Downgradient of this zone is an outer anaerobic zone where denitrification, rather than sulphate reduction, is the dominant degradation pathway; here benzene is efficiently degraded but MTBE is not. In this outer anaerobic zone, sulphate concentrations in fracture waters are rapidly re-established, by efficient equilibration (through diffusion) with the aquifer matrix pore-water and dispersive mixing with uncontaminated groundwater. This process also acts to re-supply nitrate to the fracture

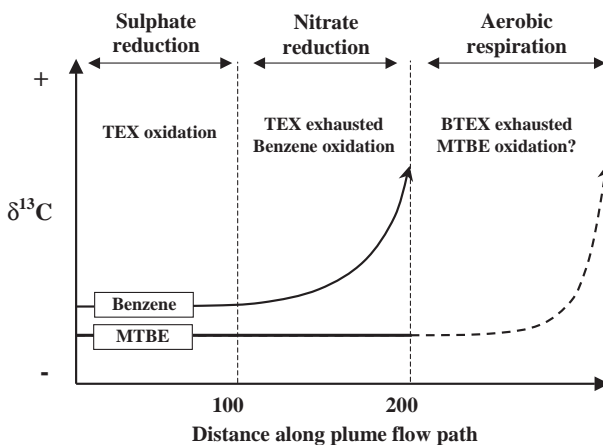


Fig. 13. Diagram summarising carbon isotopic effects associated with BTEX utilisation for different redox environments along the plume flow path. Dashed line shows hypothetical enrichment for expected MTBE degradation pathway.

waters, but fracture water nitrate concentrations remain low due to consumption by denitrification. In both anaerobic zones, degradation via manganese and iron reduction is negligible due to the limited availability of these oxides in the aquifer matrix.

For the majority of petroleum hydrocarbons, it is the availability of the electron acceptors nitrate and sulphate in the Chalk groundwater that limits biodegradation. By contrast, benzene is not degraded until competition for electron acceptors from other hydrocarbons has diminished and significant concentrations of nitrate have been restored. In the dual-porosity Chalk aquifer re-supply of electron acceptors stored in the matrix groundwater, by diffusive exchange, thus provides a fundamental constraint on degradation rates and plume development. There is no evidence for significant MTBE degradation under anaerobic conditions and in the presence of BTEX components. Further downgradient, where BTEX has been largely degraded and dissolved oxygen is once more available conditions suitable for MTBE degradation may exist (Fig. 13).

Acknowledgement

This work was sponsored by the UK Engineering and Physical Sciences Research Council, the Environment Agency and the site owner in the project: *Processes controlling the natural attenuation of fuel hydrocarbons and MTBE in the Chalk aquifer*. Rob Newton, Dave Hatfield, Andy Fairburn and Fiona Hurst provided invaluable assistance with many of the isotopic analyses. Two anonymous reviewers provided constructive comments, which have improved this paper. We thank the site owner for providing access to the site and assistance in the completion of this research.

References

- Bishop, P.K., 1990. Precipitation of dissolved carbonate species from natural-waters for Delta-C-13 analysis—a critical appraisal. *Chem. Geol.* 80 (3), 251–259.
- Bottcher, J., Strelow, O., Voerkelius, S., Schmidt, H.L., 1990. Using isotope fractionation of nitrate nitrogen and nitrate oxygen for evaluation of microbial denitrification in a sandy aquifer. *J. Hydrol.* 114 (3–4), 413–424.
- Bottrell, S.H., Spence, M.J., 2003. Using stable isotope fractionations to monitor in-situ biodegradation processes. *Bioremediation: A Critical Review*. Horizon Scientific Press.
- Bottrell, S.H., Hayes, P.J., Bannon, M., Williams, G.M., 1995. Bacterial sulfate reduction and pyrite formation in a polluted sand aquifer. *Geomicrobiol. J.* 13 (2), 75–90.
- Boutton, T.W., 1991. Stable carbon isotope ratios of natural materials: II. Atmospheric, terrestrial, marine and freshwater environments. In: Coleman, D.C., Fry, B. (Eds.), *Carbon Isotope Techniques*. Academic Press, San Diego, pp. 173–185.
- Chambers, L.A., Trudinger, P.A., 1979. Microbiological fractionation of stable sulfur isotopes: a review and critique. *Geomicrobiol. J.* 1, 249–293.
- Chapelle, F.H., et al., 1995. Deducing the distribution of terminal electron-accepting processes in hydrologically diverse groundwater systems. *Water Resour. Res.* 31 (2), 359–371.
- Craig, H., 1957. Isotopic standards for carbon and oxygen and correction factors for mass spectrometric analysis of carbon dioxide. *Geochim. Cosmochim. Acta* 12, 133–149.
- Einarson, M.D., Cherry, J.A., 2002. A new multilevel ground water monitoring system using multichannel tubing. *Ground Water Monit. Remediat.* 22 (4), 52–65.

- Fritz, P., Basharmal, G.M., Drimmie, R.J., Ibsen, J., Qureshi, R.M., 1989. Oxygen isotope exchange between sulfate and water during bacterial reduction of sulfate. *Chem. Geol.* 79 (2), 99–105.
- Hubner, H., 1986. Isotope effects of nitrogen in the soil and biosphere. In: Fritz, P., Fontes, J.-Ch. (Eds.), *Handbook of Environmental Isotope Geochemistry*. Elsevier, Amsterdam, pp. 361–425.
- Hunkeler, D., Andersen, N., Aravena, R., Bernasconi, S.M., Butler, B.J., 2001a. Hydrogen and carbon isotopic fractionation during aerobic biodegradation of benzene. *Environ. Sci. Technol.* 35 (17), 3462–3467.
- Hunkeler, D., Butler, B.J., Aravena, R., Barker, J.F., 2001b. Monitoring biodegradation of methyl tert-butyl ether (MTBE) using compound-specific carbon isotope analysis. *Environ. Sci. Technol.* 35 (4), 676–681.
- Kuder, T., Philp, P., Allen, J., Wilson, J.T., Kaiser, P., Kolhatkar, R., 2005. Enrichment of stable carbon and hydrogen isotopes during anaerobic biodegradation of MTBE: microcosm and field evidence. *Environ. Sci. Technol.* 39 (1), 213–220.
- Louie, P.K.K., Bottrell, S.H., Steedman, W., Kemp, W., Bartle, K.D., Taylor, N., 1993. A comparison by stable-isotope mass-spectrometry of coal oil coprocessing under severe-hydro-treatment and thermal conditions. *Fuel* 72 (11), 1507–1513.
- Lyngkilde, J., Christensen, T.H., 1992. Redox zones of a landfill leachate pollution plume (Vejen Denmark). *J. Contam. Hydrol.* 10 (4), 273–289.
- Mancini, S.A., et al., 2003. Carbon and hydrogen isotopic fractionation during anaerobic biodegradation of benzene. *Appl. Environ. Microbiol.* 69 (1), 191–198.
- Mariotti, A., et al., 1981. Experimental-determination of nitrogen kinetic isotope fractionation—some principles—illustration for the denitrification and nitrification processes. *Plant Soil* 62 (3), 413–430.
- McCarthy, M.D.B., Newton, R.J., Bottrell, S.H., 1998. Oxygen isotopic compositions of sulphate from coals: implications for primary sulphate sources and secondary weathering processes. *Fuel* 77 (7), 677–682.
- Mizutani, Y., Rafter, T.A., 1969. Oxygen isotopic composition of sulphates: Part 4. Bacterial fractionation of oxygen isotopes in reduction of sulphate and in the oxidation of sulphur. *N.Z. J. Sci.* 12, 60–68.
- Postma, D., Jakobsen, R., 2000. Characterisation of redox conditions in aquifers. In: Bjerg, P.L., Engesgaard, P., Krom, T.D. (Eds.), *Ground-water 2000. Proc. Int. Conf. On Ground-water Research*. Balkema, Rotterdam, pp. 207–208.
- Silva, S.R., Kendall, C., Wilkinson, D.H., Ziegler, A.C., Chang, C.C.Y., Avanzino, R.J., 2000. A new method for collection of nitrate from fresh water and the analysis of nitrogen and oxygen isotope ratios. *J. Hydrol.* 228 (1–2), 22–36.
- Spence, M.J., Bottrell, S.H., Thornton, S.F., Lerner, D.N., 2001. Isotopic modelling of the significance of bacterial sulphate reduction for phenol attenuation in a contaminated aquifer. *J. Contam. Hydrol.* 53 (3–4), 285–304.
- Strebel, O., Bottcher, J., Fritz, P., 1990. Use of isotope fractionation of sulfate–sulfur and sulfate–oxygen to assess bacterial desulfurification in a sandy aquifer. *J. Hydrol.* 121 (1–4), 155–172.
- Thornton, S.F., Quigley, S., Spence, M.J., Banwart, S.A., Bottrell, S.H., Lerner, D.N., 2001. Processes controlling the distribution and natural attenuation of dissolved phenolic compounds in a deep sandstone aquifer. *J. Contam. Hydrol.* 53 (3–4), 233–267.
- Wealthall, G.P., Thornton, S.F., Lerner, D.N., 2002. Assessing the transport and fate of MTBE-amended petroleum hydrocarbons in the UK Chalk aquifer. In: Thornton, S.F., Oswald, S.O. (Eds.), *GQ2001: Natural and Enhanced Restoration of Groundwater Pollution*, Sheffield, U.K., 16–21 June 2001. IAHS Publ. No. 275, 205–212.